



The influence of subtropical cold fronts on the surface energy balance of a semi-arid site

Jason Beringer* & Nigel J. Tapper

Department of Geography and Environmental Science, Monash University, Melbourne, Australia

(Received 7 May 1999, accepted 28 October 1999)

The passage of subtropical cold fronts through central Australia produces the only significant mesoscale meteorological features in the region. The interaction of these cold fronts with the surface energy balance strongly affects the local weather and climate. The surface energy balance was measured at a semi-arid site in Alice Springs, central Australia, to determine how it was influenced by the passage of subtropical cold fronts. Both Bowen ratio and eddy correlation methods were used. The daytime energy balance of the site showed high net radiation that was partitioned into 75% sensible heat flux and 25% soil heat flux with little or no latent heat flux. At night there was a large net radiative loss that was balanced primarily by a loss of heat from the soil. The cold fronts predominately passed through Alice Springs at night and showed a strong surface signature. The fronts brought moister air resulting in higher water vapour pressures during their passage. The nocturnal boundary layer was often disturbed as the front passed, resulting in warm, moist air being mixed down toward the land surface. Mixing decreased the soil heat flux and increased latent heat fluxes toward the surface. Moisture that accumulated at the surface at these times was often evaporated after a return to drier conditions. During the daytime, surface signatures in soil and sensible heat fluxes were less distinct due to the strong convective mixing. Latent heat fluxes followed a similar trend to the nocturnal case.

© 2000 Academic Press

Keywords: surface energy exchange; climate dynamics; subtropical cold fronts; boundary layer; central Australia; Alice Springs; semi-arid regions

Introduction

The receipt of incoming net radiation at the earth's surface provides the primary source of energy in the surface energy balance. At the surface, net radiation is predominately partitioned into the turbulent fluxes of heat and moisture and heat conducted into the soil substrate. Exchanges of energy at the surface have a profound influence on the local- and regional-scale climate and synoptic-scale meteorological features. For example, the surface energy balance has been identified as being important in the generation of synoptic-scale North Australian Cloud Lines over the Cape York Peninsula (Tapper & Barta, 1992), locally generated mesoscale circulations over dry salt lakes (Tapper, 1991), boundary-layer development over native *vs.* non-native vegetation (Lyons *et al.*, 1993) and the evolution of subtropical cold fronts (Cleugh & Roberts, 1994).

Given that 70% of Australia's land area is semi-arid (annual rainfall < 250 mm) (Cleugh & Roberts, 1994), a quantitative knowledge of climate processes including energy exchanges and synoptic-scale climate dynamics is important for use in analysis and forecasting of weather in the central Australian region. Subtropical cold fronts are the most significant meteorological feature affecting central Australia and it is the surface energy exchanges that are vital in modulating their characteristics and behaviour (Smith *et al.*, 1995). In particular, the nocturnal energy balance is essential in developing a radiational inversion that modifies the passage of the frontal system. The interactions of cold fronts with the surface energy exchanges are of fundamental meteorological interest and will aid in the development and parameterization of both regional and larger-scale numerical models. Neither the surface energy exchanges nor the synoptic features of the semi-arid regions of central Australia have been well characterized, mainly due to a lack of observations throughout this sparsely populated area.

Despite the importance of surface energy exchanges in driving climate in the region, there have been few studies examining the surface exchanges of energy in semi-arid regions, especially in Australia. However, some direct observations of the surface energy balance and radiation budget have been presented by Cleugh & Roberts (1994) for a site in central Australia close to Alice Springs. Moreover, there is a paucity of knowledge on how synoptic scale features such as cold fronts may influence the surface energy balance in any region. A series of field experiments has previously examined frontal structure and dynamics in central Australia. This series of field experiments began with a small-scale pilot experiment that was conducted during September 1988 in the Mt. Isa region (Smith & Ridley, 1990). Following this, the first Central Australian Fronts Experiment (CAFE91) took place in 1991 (Smith *et al.*, 1995; Deslandes *et al.*, in press). The experiment investigated the structure and behaviour of subtropical cold fronts that affect central and north eastern Australia. It also investigated the interaction of fronts with the developing nocturnal inversion and the generation of propagating bore-like or solitary wave disturbances (Smith *et al.*, 1995). The crest of these waves often produces spectacular roll clouds, or a succession of roll clouds that occur early in the morning, most frequently toward the end of the dry season, in the southern part of the Gulf of Carpentaria region of northern Australia (Smith, 1988). This phenomenon is locally known as a 'morning glory'. Reviews of the morning glory phenomena can be found in Smith (1988) and Christie (1992).

Building on this previous work, a second field experiment was undertaken during 1996, and was called the Central Australia Fronts Experiment 1996 (CAFE96). The experiment was organized jointly by Monash University, the Australian National University, the University of New South Wales and the University of Munich, with collaborative support from the Bureau of Meteorology's Northern Territory Regional Office. It aimed to provide detailed observational data on surface energy exchanges and their interaction with the passage of subtropical cold fronts. In addition, the dynamical features of these fronts were examined in greater detail than was previously possible. The broad scale synoptic patterns, individual observations from a number of surface meteorological stations and prognostic analyses for individual cold fronts are documented in Reeder *et al.* (in press) and have not been repeated here. This paper focuses on quantifying the energy exchanges of this semi-arid landscape and is unique in being able to examine the interaction of the passage of subtropical cold fronts through central Australia on the surface energy exchange.

Site description

The observational network during CAFE96 comprised twelve automatic weather stations installed in the area between Alice Springs and Mt. Isa (Fig. 1). Instruments to measure the surface energy balance were installed at Alice Springs within the Bureau of

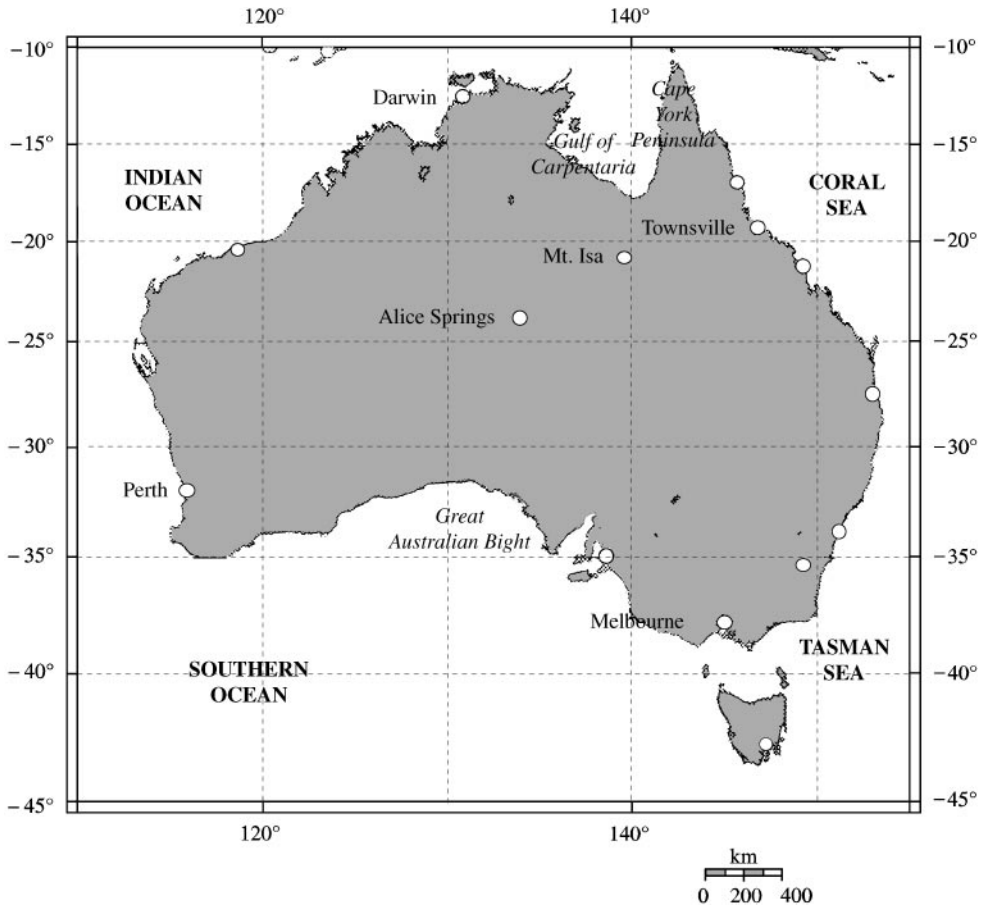


Figure 1. Map of Australia showing Alice Springs, the location of the surface energy balance measurements.

Meteorology compound of Alice Springs Airport ($23^{\circ}8'S$, $133^{\circ}9'E$). The fetch was homogeneous and greater than 500 m in all directions. The surface consisted of a dry red, sandy soil with some small scattered stones and sparse native grasses less than 20 cm tall. Surface energy balance measurements were taken over 35 days between 5 September and 10 October 1996. The time system used here is Central Standard Time (CST) which is UTC + 9.5 h.

Methodology

The incoming solar radiation is partitioned into component fluxes of latent heat, sensible heat, ground heat flux and storage terms. The energy balance of a site may be described as:

$$R_n = H + LE + S + P \quad (1)$$

where R_n is the net all-wave radiative flux, H is the sensible heat flux, LE is the latent flux, G is the soil heat flux, S is the rate of heat storage and P is the photosynthetic energy flux. Equation 1 describes how the net incoming solar radiation is partitioned into the components of latent heat flux, sensible heat flux, soil heat flux and storage terms.

A Bowen ratio system was installed at Alice Springs to measure the surface energy exchange together with an eddy correlation system that was operated for part of the time. In both systems net radiation was measured at a height of 2 m using a net radiometer (Radiation and Energy Balance Systems, model Q7.1) to which a dynamic wind correction was applied to correct for convective cooling of the net radiometer domes. The soil heat flux (G) was calculated using the combination method (Fritschen & Simpson, 1989). The method assumes that G can be expressed as the heat flux at a depth of 8 cm ($G_{8\text{cm}}$) below that surface plus heat storage above the heat flux plate:

$$G = G_{8\text{cm}} + \frac{C_s d \Delta T_s}{t} \quad (2)$$

The soil heat flux at 8 cm was measured using two heat flux plates (Radiation and Energy Balance Systems, model HFT3). Storage above the heat flux plate was calculated using the heat capacity of soil (C_s) and measuring the change in temperature (ΔT_s) of the soil layer above the heat flux plate ($d = 0.08$ m) over a 20 min period ($t = 1200$ s) (Oke, 1987). The average soil temperature was measured using a soil averaging thermocouple (Campbell Scientific, model TCAV) above each plate with thermocouples placed at 2 and 6 cm below the surface. The specific heat of the soil was assumed to be $1.29 \times 10^6 \text{ J m}^{-3} \text{ K}^{-1}$ (Oke, 1987). The water content is very small in this semi-arid sandy soil and was not quantified during the study. In this study both the storage in the air layer between the surface and the instruments and the energy used in photosynthesis is assumed to be negligible (Wang & Mitsuta, 1992) and has been neglected.

The Bowen ratio technique

The Bowen ratio technique for determining the partitioning of energy into sensible and latent heat fluxes was first described by Bowen (1926). The technique uses the Bowen ratio (β) to partition the available energy ($R_n - G - S - P$) into the turbulent fluxes of heat and moisture. The Bowen ratio is defined as the ratio of sensible heat flux to latent heat flux:

$$\beta = \frac{H}{LE} \quad (3)$$

The Bowen ratio can be determined by measuring the ratio of the difference in vapour pressure and temperature between two heights. In this study a commercial Bowen ratio system (Campbell Scientific) was used to measure the temperature and vapour pressure differences between two fixed heights on a tripod (Beringer & Tapper, 1996). The arms were installed at 1.15 and 3.1 m above the surface and were oriented at 200° magnetic in the direction of the prevailing wind. Temperature was measured using chromel-constantan thermocouples (resolution 0.006°C), while vapour pressure was calculated from dew point temperature (resolution of 0.05°C) measured using a cooled mirror dew point hygrometer. The temperature and vapour pressure were measured every second and averaged over each 20-min period and stored on a datalogger that also controlled the Bowen ratio system (Campbell Scientific, model 21X).

The eddy correlation technique

The eddy correlation technique measures vertical fluxes of scalar properties such as heat, water, CO_2 and momentum by measuring the short-term turbulent fluctuations

around their longer-term mean. The vertical flux density (F) of an entity (s) is F_s and is given by:

$$F_s = \overline{(\bar{\rho} + \rho')(\bar{w} + w')(\bar{s} + s')}, \quad (4)$$

where ρ is the scalar density, w is the vertical velocity and s is the volumetric content of the scalar (i.e. temperature, water vapour, CO₂). An overbar ($\bar{\quad}$) indicates the time average of the instantaneous values (primed'). With the assumptions that the mean vertical velocity is zero, the relation in the underlying eddy correlation approach is then:

$$F_s = \overline{\rho w' s'}. \quad (5)$$

The overbar in this equation denotes the time average of the instantaneous covariance of w and s and is hence often referred to as the eddy covariance method. Sensible and latent heat fluxes can be written as:

$$H = \rho C_p \overline{w' T'}, \quad (6)$$

$$\text{and } LE = L_v \overline{w' p'_v}. \quad (7)$$

For this project, the vertical wind velocity was measured with a 1-dimensional sonic anemometer (Campbell Scientific, model CA27), while the temperature and vapour pressure were measured with a fine wire thermocouple (Campbell Scientific, model 127) and krypton hygrometer (Campbell Scientific, model KH20), respectively. These signals were sampled at 10 Hz, although only the 20-min means, variances, covariances and correlations were recorded. These measurements were also used to calculate the fluxes in real time. The sensors were mounted 2.125 m above the ground and were separated 15 cm horizontally. The eddy correlation system was operated for selected periods during the experiment.

Results

The surface energy balance at a semi-arid site (Alice Springs)

A comparison of sensible heat fluxes from 10 consecutive days of data (8–18 September) between Bowen ratio and eddy correlation data showed a good correlation between sensible heat flux from the two systems ($r^2 = 0.97$, data not shown). The eddy correlation system underestimated sensible heat flux by 36% in comparison to the Bowen ratio system. The latent heat fluxes were generally so small in magnitude that they showed no clear trend in over or under estimation. An examination of the surface energy balance for a typical day portrays the underestimation of sensible heat fluxes in the eddy correlation method but also the good correlation in flux trends calculated using both the eddy correlation and Bowen ratio systems (Fig. 2).

The lack of closure in the energy balance equation (closure = $R_n - G - H - LE$) for the eddy correlation system on a daily basis (24 h) was 12% of net radiation. At night the closure was near zero, but during daylight hours ($R_n > 0$) the energy budget did not close by an average of 29%. This large non-closure resulted in around 170 Wm^{-2} of energy not accounted for at midday (12 00 CST). The reason for the lack of closure is unclear but unlikely due to storage terms or incorrect parameterization of the soil heat flux. At night, when the soil heat flux is the dominant source of heat, and turbulent fluxes are small, the energy balance closure is almost 100%. Advection is also unlikely given the large uniform area of short grass vegetation. As the soil heat flux is well characterized and the latent heat fluxes are small the lack of closure is likely to be due to an underestimation of sensible heat flux. The lack of closure during the daytime (29%) is almost matched by the underestimation of sensible heat flux (26%). The underestimation of sensible heat flux could be due to limitations in the frequency response of the system (10 Hz).

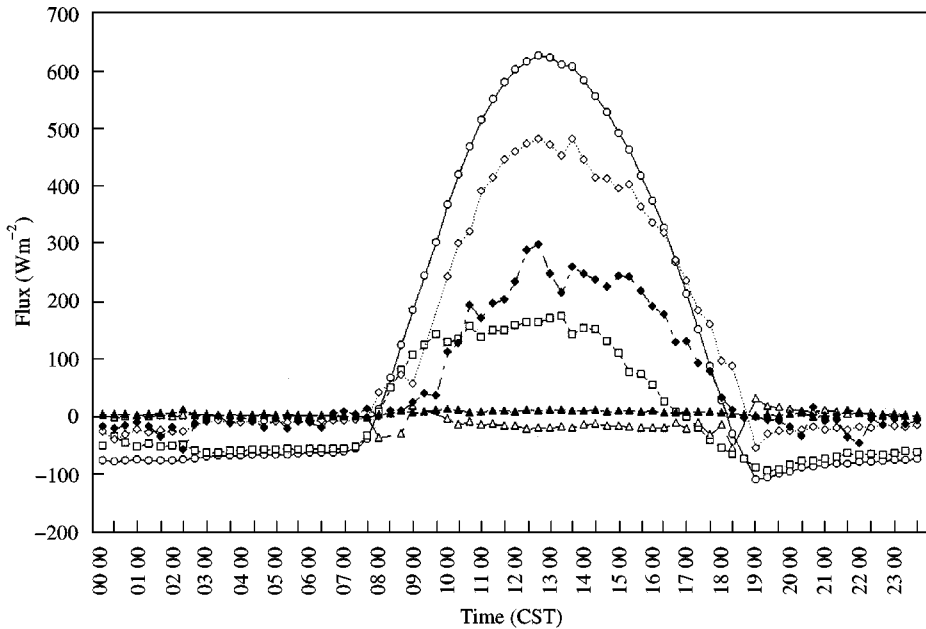


Figure 2. A typical diurnal energy balance for both eddy correlation and Bowen ratio system on 8 September 1996: $\text{---}\circ\text{---}$ R_n ; $\text{---}\square\text{---}$ G ; $\text{---}\diamond\text{---}$ H (Bowen ratio system), $\text{---}\triangle\text{---}$ LE (Bowen ratio system); $\text{---}\blacklozenge\text{---}$ H (Eddy correlation system); $\text{---}\circ\text{---}$ LE (Eddy correlation system).

In addition to the general underestimation of sensible heat flux by the eddy correlation system, a comparison of fluxes during cold front events showed a very large increase in the lack of closure of the energy balance. This is likely to be due to the effect of the cut-off time scale on the calculation of fluxes. The cut-off time scale defines the averaging time over which mean components are obtained in order to partition entities into mean and perturbation components (Sun *et al.*, 1996). In the presence of significant mesoscale activity, such as cold fronts, the mean components can be greatly influenced by the passage of a significantly different air mass and hence also affect the calculated turbulent fluxes (Sun *et al.*, 1996). The future use of the eddy correlation system and data processing for experiments such as this should store the raw turbulence velocity and scalar data in order to allow analysis of turbulent spectra and cospectra and to better diagnose potential errors.

The poor closure in the eddy correlation system and the increase in closure during cold front events cause some concern for the validity of the eddy correlation measurements. Given this poor closure and the extensive use of the Bowen ratio system throughout the experiment, only the later measurements are presented. This also allows better visualization of the flux data.

The general trends in the surface energy balance are shown in Fig. 3 (radiative fluxes are given as positive into the surface while other fluxes are positive away from the surface). The salient features of the surface energy balance are the high net radiation during the day brought about by a high shortwave solar input and moderate albedo (Fig. 3). Although the surface albedo was not directly measured at this site, Cleugh & Roberts (1994) measured an albedo of 17.4% over a similar red sandy soil type at a site close to Alice Springs.

The soil was extremely dry throughout the measurement period, which resulted in virtually no latent heat fluxes (Fig. 2). Sensible heat is therefore the dominant energy sink during the day and accounts for around 75% of net radiation at midday (Fig. 2). The

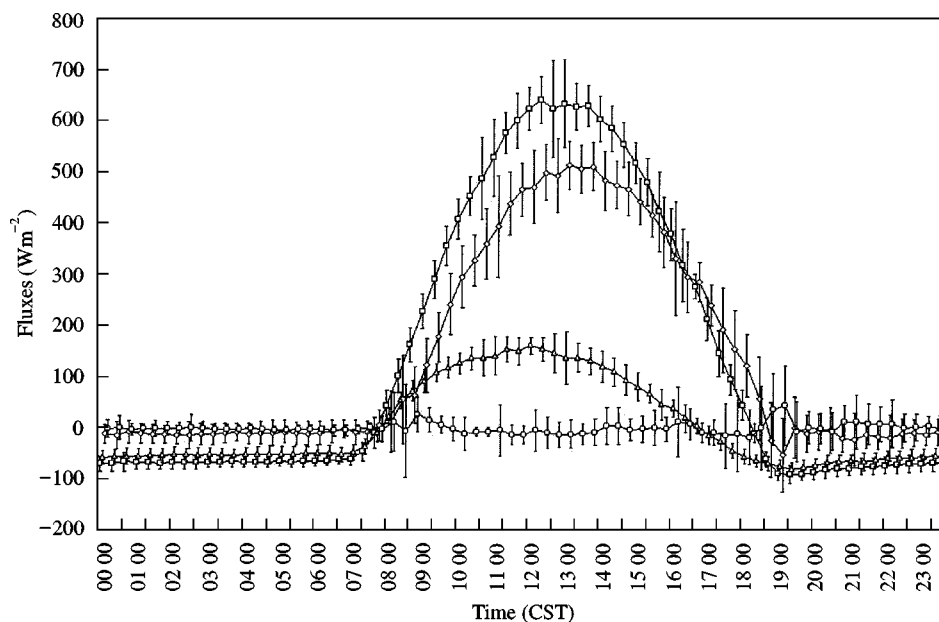


Figure 3. Composite diurnal energy balance for Alice Springs using Bowen ratio measurements (means and standard deviations of 20 intervals) (5 September to 10 October): \square R_n ; \triangle G ; \diamond H ; \circ LE .

soil heat flux is also very large due to the high radiational input and the sparseness of vegetation at the site. The soil heat flux accounts for the remaining 25% of net radiation. The relatively low thermal diffusivity for soils of this type ($2.21 \text{ m}^2 \text{ s}^{-1}$ (Cleugh & Roberts, 1994)) results in high day time soil temperatures. During night time the net radiation is strongly negative due primarily to longwave radiational losses typical of arid regions (Smith *et al.*, 1986). The loss of net radiation at night also results in a strong flux of heat out of the soil.

The aridity of the site, as well as the thermal properties of the soil, controls the partitioning of the radiative energy into the various heat fluxes. These general trends are typical of other arid and semi-arid sites (Kustas *et al.*, 1991; Cleugh & Roberts, 1994).

The influence of cold front passage on surface energy exchanges

During CAFE96 seven cold frontal passage events were documented of which three frontal systems are examined in detail. There is a strong propensity for cold fronts to pass through Alice Springs during nocturnal hours (Smith *et al.*, 1995), and hence two nocturnal cases are examined. Event 2 represents a typical nocturnal passage of a subtropical cold front. Event 3 illustrates another nocturnal passage but a case where the cold front weakened some 4 h after the initial passage. The third case represents a less typical early morning passage of a cold front (event 5). The trends in the energy balance components and meteorological variables for these three events are shown in Table 1.

CAFE event 2

Event 2 was a nocturnal event occurring between 4–5 September and was defined by the passage of a weak frontal system through central Australia. A ridge of high pressure over

Table 1. Trends in the surface energy exchanges during the initial cold front passage. (NC = no change; \uparrow = increase in magnitude; \downarrow = decrease in magnitude; $-ve$ = flux is away from the surface; $+ve$ = flux is towards the surfaces. T_a = air temperature; T_s = soil temperature; VP = vapour pressure).

| Event | Date | Time | R_n | G | H | LE | T_a | T_s | VP |
|-------|---------|-------|----------------|------------------|----------------|---------------|------------|------------|------------|
| 2 | 4-5/9 | Night | $\uparrow -ve$ | $\downarrow -ve$ | $\uparrow -ve$ | + ve to $-ve$ | \uparrow | \uparrow | \uparrow |
| 3 | 11-12/9 | Night | $\uparrow -ve$ | $\downarrow -ve$ | $\uparrow -ve$ | + ve to $-ve$ | \uparrow | \uparrow | \uparrow |
| 5 | 23/9 | Day | NC | NC | NC | $-ve$ | NC | NC | \uparrow |

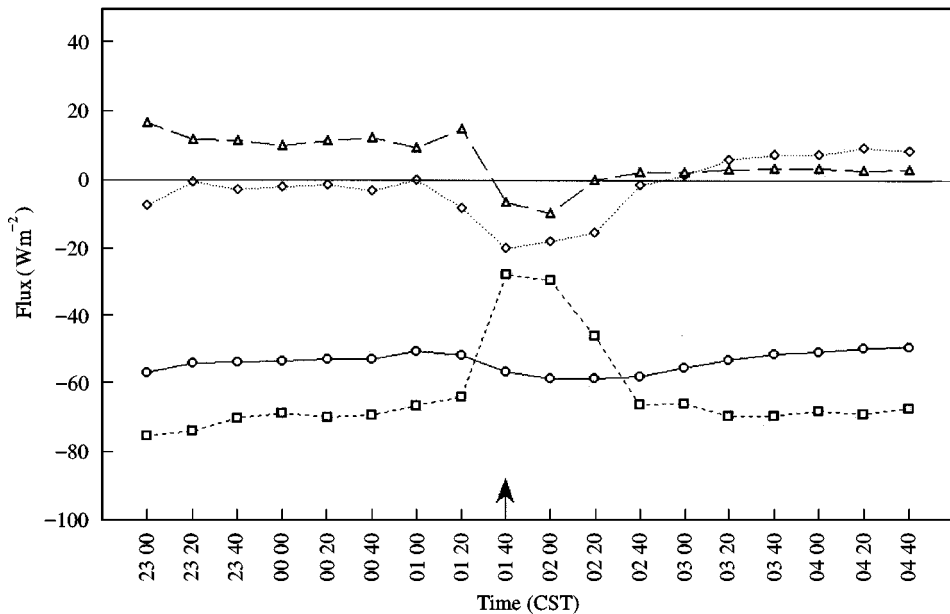


Figure 4. Surface energy balance for event 2. The arrows show the timing of the frontal passage and other significant events. $-\circ-$ R_n ; $-\square-$ G ; $-\diamond-$ H , $-\triangle-$ LE .

eastern Australia dominated the continent and a low over the Tasman Sea was moving steadily to the south-east and weakening. A weak front passed through Alice Springs at 0140 CST on 5 September (Fig. 4) and was typical of all the observed nocturnal events in that the frontal air mass was moister than the nocturnal air mass it replaced. There was therefore an increase in water vapour pressure associated with the passage of the cold front in each of the three cases presented.

The nocturnal energy balance in the two hours prior to the frontal passage at 0140 CST showed a high average net radiation of -50 Wm^{-2} (Fig. 4). The significant loss of net radiation at night produces a nocturnal radiation inversion and a stable and probably shallow boundary layer. The nocturnal radiation inversion was also documented by Smith *et al.* (1995) during CAFE 91. The development of this surface based radiation inversion is important because large amplitude internal bore waves that are generated in association with the cold front propagate on the shallow inversion and are partially trapped by the deep, well-mixed layer above (Reeder *et al.*, in press). The bore waves are closely linked with the formation of the southerly 'morning glories' but dissipate

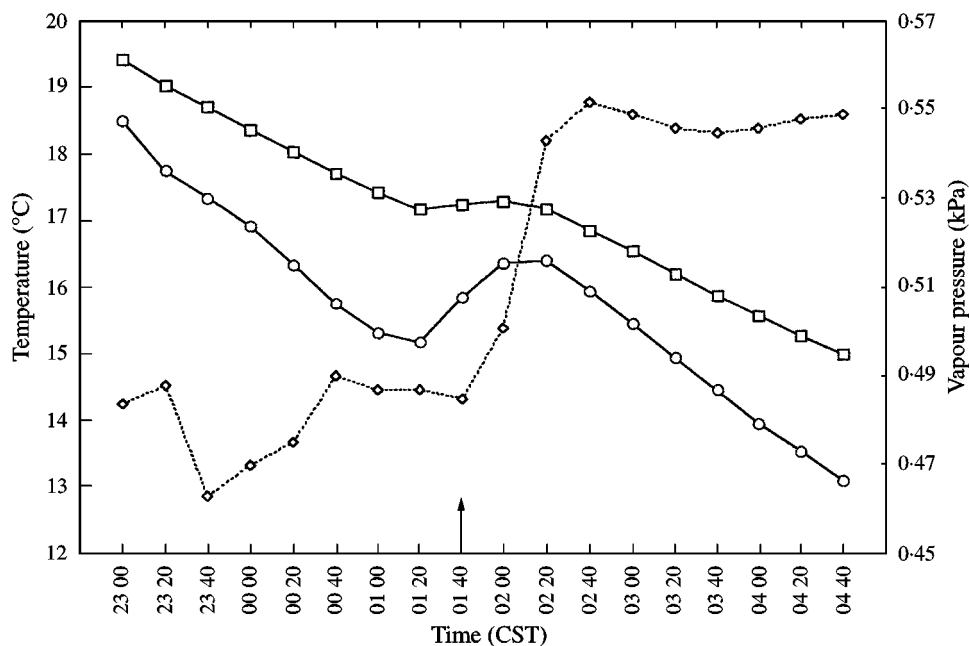


Figure 5. Ambient meteorological conditions during event 2. The arrows show the timing of the frontal passage and other significant events. —○— Air temperature; —□— soil temperature; —◇— vapour pressure (2 m).

shortly after sunrise when convective mixing destroys the nocturnal inversion (Reeder *et al.*, in press).

The radiational loss that generated the radiation inversion was balanced primarily by a large heat loss from the soil averaging -70 W m^{-2} between 23 00 and 01 40 CST (Fig. 4). The remaining available energy ($R_n - G$) for partitioning into the turbulent fluxes was small and positive which assisted in driving the positive values of latent heat fluxes (around $+10 \text{ W m}^{-2}$) (Fig. 4). The source of this moisture is unclear, but the flux is associated with an increase in the vapour pressure gradient in the stable boundary layer. However, the environment was still arid as evidenced by the Bowen ratio (H/LE) of around 4.

Changes in the energy balance and meteorological measurements due to the frontal passage past the station were evident at 01 40 CST. At this time the rate of change in air temperature reversed from negative to positive (Fig. 5). The front disturbed the nocturnal boundary layer and mixed warmer and moister air toward the surface. Consequently, between 01 40 and 02 20 CST there was an increase in the air temperature and vapour pressure compared to prefrontal conditions (Fig. 5). The downward mixing of air also reduced the temperature gradient between the soil and the air that reduced the loss of heat flux from the ground (Fig. 4).

The net radiation losses increased by 8 W m^{-2} during the frontal passage from 51 W m^{-2} at 01 20 CST to 59 W m^{-2} at 02 00 CST (Fig. 4). This was also associated with a 0.25°C increase in surface soil temperature (Fig. 5) that would serve to increase the outgoing longwave radiation and hence account for part of the radiational losses. Using the Stefan-Boltzman Law and assuming a surface emissivity of one, the contribution of this mechanism may be calculated to be approximately 1.5 W m^{-2} . The remaining 6.5 W m^{-2} increase in negative net radiation could be brought about by a decrease in

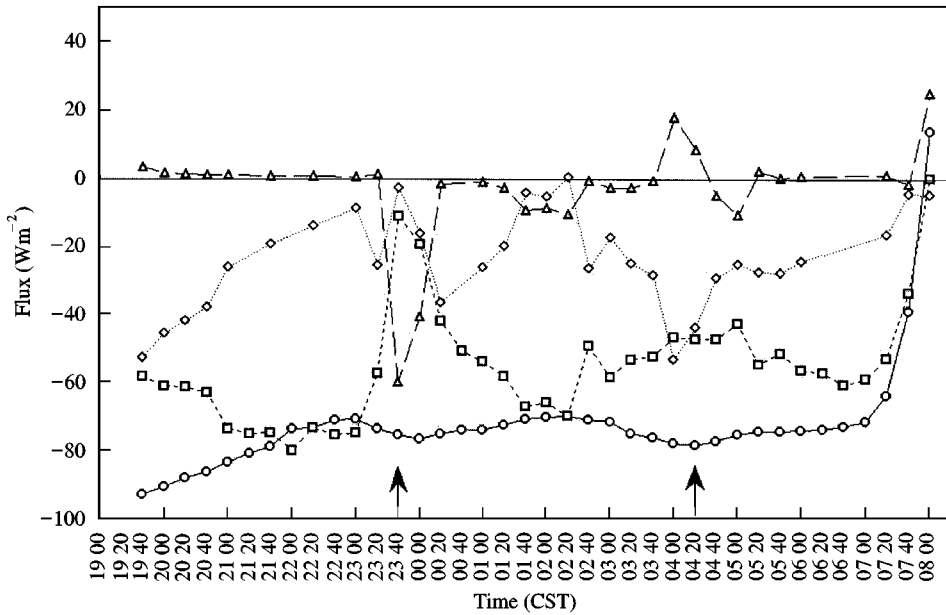


Figure 6. Surface energy balance for event 3. The arrows show the timing of the frontal passage and other significant events. —○— R_n ; —□— G ; ···◇··· H , —△— LE .

incoming longwave radiation. This is most likely to be due to the establishment of a much colder overlying air mass behind the cold front.

For the period between 01 40 and 02 20 CST the available energy ($R_n - G$) for partitioning into the turbulent fluxes was less than zero. This caused both latent and sensible heat fluxes to become negative during this time (Fig. 4). The negative latent heat flux means that the atmospheric water vapour was directed toward the surface.

After 02 40 CST the soil heat flux returned to prefrontal values of around -70 W m^{-2} and the available energy became positive again (Fig. 4). An examination of the Bowen ratio during this time shows a large increase from 4 to around 15 that portrays an increasing aridity after the initial disturbance associated with the frontal passage.

CAFE event 3

Event 3 represents a different nocturnal event that occurred between 11–12 September and passed through Alice Springs at 23 40 CST. Event 3 differed from event 2 in that there was an observed weakening of the front that occurred 4 h later at 04 20 CST. A trough with a well-developed vertical structure that had developed from a deep low over the Great Australian Bight and a weakening ridge over eastern Australia produced this front.

Prior to 20 00 CST and the arrival of the front, the energy balance was typical of previous nocturnal energy regimes for this semi-arid site (Fig. 2). Latent heat fluxes remained small but positive and sensible heat fluxes were moderately negative (Fig. 6). The net radiation was relatively consistent throughout the night averaging -75 W m^{-2} (Fig. 6). As in event 2, there was a slight increase in net radiation associated with the frontal passage (Fig. 6).

The frontal passage again resulted in the downward mixing of warm and moist air at the frontal edge which served to stabilize and even slightly increase the air and soil temperatures in an otherwise steadily decreasing temperature pattern (Fig. 7). This

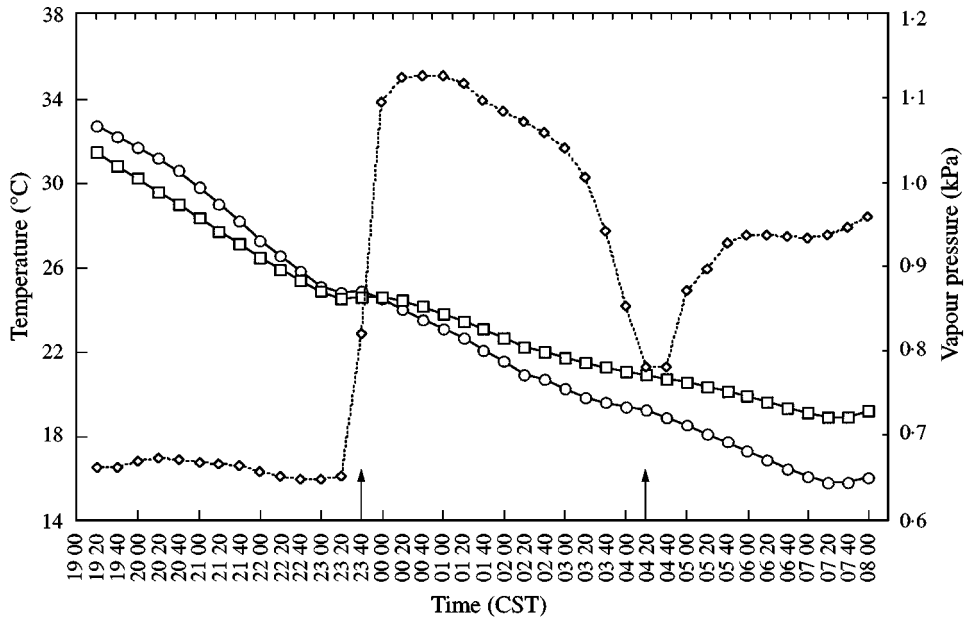


Figure 7. Ambient meteorological conditions during event 3. The arrows show the timing of the frontal passage and other significant events: —○— Air temperature (2 m); —□— soil temperature; —◇— vapour pressure (2 m).

reduced the soil-to-air temperature gradient and there was subsequently a small change in the rate of soil temperature decline. This affected the soil heat storage leading to a temporary decrease in the magnitude of the soil heat flux from -70 at 23 00 CST to -10 Wm^{-2} at 23 40 CST (Fig. 6).

Between 23 40 and 00 00 CST there was a large increase in the atmospheric water vapour pressure (0.65 to 1.1 kPa) associated with the disturbed frontal air (Fig. 7). This moist air is consistent with the moist air mass seen in event 2. There is hence a movement of water vapour to the very dry soil that results in a large negative latent heat flux (-60 Wm^{-2}) for a short period (Fig. 6).

The immediate effect of the front was evident for around 40 min and had a large impact on the nocturnal energy balance as the stable nocturnal boundary layer was disrupted during this time. At 04 20 CST there was a weakening of the frontal influence and a return to a drier air mass (Fig. 7). As a result, the water vapour that had been absorbed into the soil substrate was released, resulting in a positive latent heat flux of 20 Wm^{-2} out of the surface (Fig. 6). This was partially balanced by an increase in the sensible heat flux toward the surface as the stable boundary layer was rebuilt.

CAFE event 5

Event 5 (23 September) is an example of the morning passage of a weak cold front. The synoptic situation for this event showed a weak high persisting over the Coral Sea while another high-pressure ridge moved into western Australia. This ridge followed behind a trough associated with a cold front moving across the continent. The cold front moved through the region to the south-west of Alice Springs and slowed down during the day due to the convective mixing of the boundary layer. The high-pressure system over the Coral Sea maintained a supply of moist air ahead of the trough. The moist air associated with the approach and passage of the front was evident in the measurements

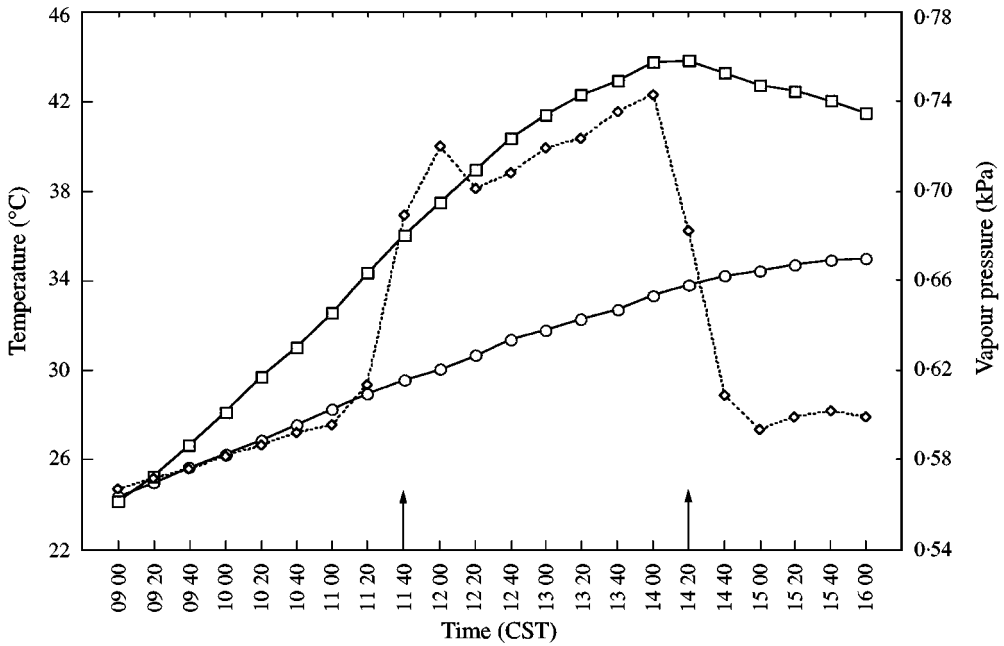


Figure 8. Ambient meteorological conditions during event 5. The arrows show the timing of the frontal passage and other significant events: —○— Air temperature (2 m); —□— soil temperature; —◇— vapour pressure (2 m).

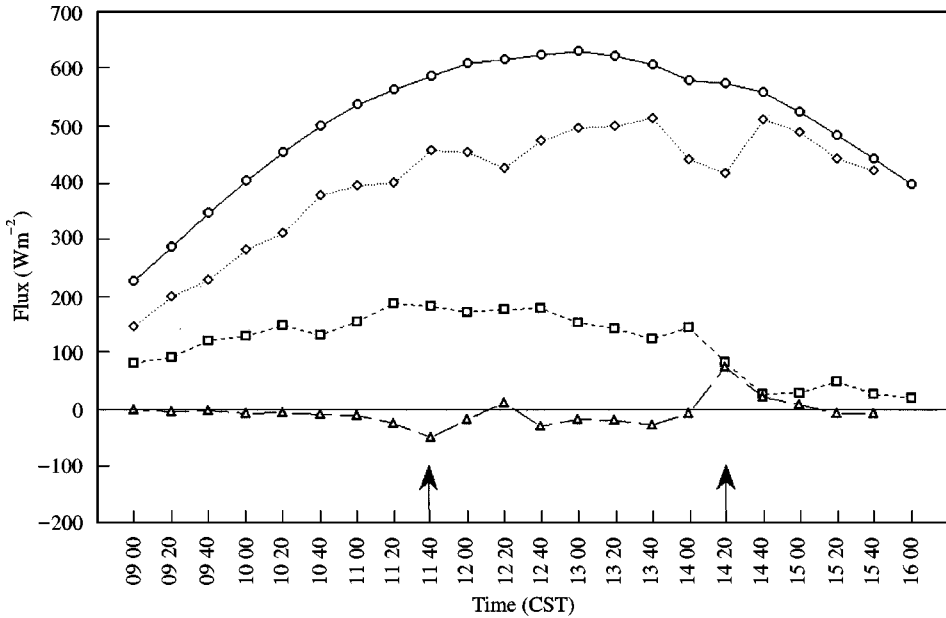


Figure 9. Surface energy balance for event 5. The arrows show the timing of the frontal passage and other significant events: —○— R_n ; —□— G ; —◇— H ; —△— LE.

as an increase in vapour pressure from 0.61 to 0.69 kPa at 11 40 CST (Fig. 8). The increase in vapour pressure caused atmospheric moisture to be transferred from the air to the surface. This resulted in a moderately strong negative latent heat flux of -51 Wm^{-2} at 11 40 (Fig. 9).

The high input of net radiation and subsequent large sensible heat fluxes created strong convective turbulent mixing that resulted in air temperature, soil heat flux and sensible heat flux remaining virtually unchanged by the frontal passage (Fig. 9). During CAFE91 subtropical cold fronts were often difficult to locate during the early morning and afternoon when surface heating produced a peak in convective mixing (Smith *et al.*, 1995). The other observed daytime frontal passage (event 4) showed no discernible change in the surface energy balance (data not shown).

After 12 00 CST, the energy balance recovered until 14 40 CST when the moist air associated with the frontal passage moved past the station, allowing a return to drier conditions in the air mass behind the front (Fig. 8). The moisture that had been transferred to the soil during the passage of moist frontal air was released to the atmosphere and the latent heat fluxes changed from -7 Wm^{-2} in the 20 min period preceding 14 40 CST to $+74 \text{ Wm}^{-2}$ (Fig. 9). As a result of the increased moisture availability and partitioning of energy into latent heat flux, the sensible heat decreased concurrently for a short period.

Conclusions

The passage of cold fronts across the semi-arid regions of central Australia is a common but significant synoptic feature. The surface energy exchanges in the region are important in modifying the characteristics and behaviour of the cold fronts. The general surface energy balance at Alice Springs in Central Australia was typical of other semi-arid sites and showed little or no latent heat flux, with the high net radiation being partitioned into approximately 75% sensible heat and 25% soil heat flux. The partitioning of the net radiation between these two fluxes depends primarily on the surface and soil properties.

The diurnal variations in surface energy exchange are consistent with variations in frontal structure associated with diabatic processes. Passage of cold fronts during the day time produced a less visible meteorological signature than their nocturnal counterpart and there was little evidence of changes in the sensible and soil heat fluxes. This was due to strong convective processes and a well-mixed boundary layer. However, moist air ahead of and associated with the passage of the front resulted in a transfer of moisture from the air towards the surface. After the frontal passage there was sometimes a sudden return to drier conditions as the front weakened, which resulted in the evaporation of any moisture that had accumulated at the surface. Hence, latent heat fluxes would become positive during this time.

In the evening, however, the fronts develop strong surface signatures as the radiative input is reduced and convection subsides. During nocturnal hours a surface-based radiation inversion develops and the fronts develop a stronger surface signature. The majority of cold fronts passing through Alice Springs were nocturnal and changes in the surface energy exchanges resulted from a change of the stable nocturnal air mass to a well-mixed air mass. In the CAFE96 observations, this was always accompanied by an increase in air temperature and vapour pressure due to the disturbance of the nocturnal boundary layer and a downward mixing of warm and moist air. This caused a reduction or removal of the temperature gradient between the air and soil that resulted in a strong reduction in heat loss from the soil. As for the daytime case a moist frontal air mass caused a transfer of moisture to the surface resulting in strong negative latent heat fluxes. This was often reversed after the passage of the front. Importantly, as the inversion strengthens towards the early morning a non-linear wavelike or bore-like structure

develops at the leading edge of the frontal zone (Reeder *et al.*, in press). This process is linked with the formation of the spectacular 'morning glory' that is often seen over the Gulf country.

References

- Beringer, J. & Tapper, N.J. (1996). Evapotranspiration measurement using the Campbell Scientific Bowen ratio system. *Proceedings of the Second Australian Conference on Agricultural and Forest Meteorology*, pp. 229–235 Brisbane: The University of Queensland Printer. 301 pp.
- Bowen, I.S. (1926). The ratio of heat losses by conduction and by evaporation from any water surface. *Physical Review*, **27**: 779–787.
- Christie, D.R. (1992). The morning glory of the Gulf of Carpentaria: A paradigm for nonlinear waves in the lower atmosphere. *Australian Meteorological Magazine*, **41**: 21–60.
- Cleugh, H.A. & Roberts, T. (1994). Local-scale energy balances and microclimate in the desert ranges of central Australia. *Australian Meteorological Magazine*, **43**: 219–228.
- Deslandes, R., Reeder, M.J. & Mills, G. (in press). Synoptic analyses of a subtropical cold front observed during the 1991 Central Australian Fronts Experiment. *Australian Meteorology Magazine*.
- Fritschen, L.J. & Simpson, J.R. (1989). Surface energy and radiation balance systems: General description and improvements. *Journal of Applied Meteorology*, **28**: 680–689.
- Kustas, W.P., Goodrich, D.C., Moran, M.S., Amer, S.A., Bach, L.B., Blanford, J.H., Chehbouni, A., Claassen, H., Clements, W.E., Doraiswamy, P.C., Dubois, P., Clarke, T.R., Daughtry, C.S.T., Gellman, D.I., Grant, T.A., Hipps, L.A., Huete, A.R., Humes, K.S., Jackson, T.J., Keefer, T.O., Nichols, W.D., Parry, R., Perry, E.M., Pinker Jr, R.T., Qi, J., Riggs, A.C., Schmugge, T.J., Shutko, A.M., Stannard, D.I., Swiatek, E., van Leeuwen, J.D., van Zyl, J., Vidal, A., Washburne, J. & Wertz, M.A. (1991). An interdisciplinary field study of the energy and water fluxes in the atmosphere-biosphere system over semiarid rangelands: Description and some preliminary results. *Bulletin of the American Meteorological Society*, **72**: 1683–1705.
- Lyons, T.J., Schwerdtfeger, P., Hacker, J.M., Foster, I.J., Smith, R.C.G. & Xinmei, H. (1993). Land-atmosphere interaction in a semiarid region: The Bunny fence experiment. *Bulletin of the American Meteorological Society*, **74**: 1327–1334.
- Oke, T.R. (1987). *Boundary Layer Climates*. London: Routledge. 437 pp.
- Reeder, M.J., Smith, R.K., Deslandes, R., Tapper, N.J. & Mills, G.A. (in press). Subtropical fronts and bores observed during the 1996 Central Australian Fronts Experiment. *Quarterly Journal of the Royal Meteorological Society*.
- Smith, E.A., Reiter, E.R. & Gao, Y. (1986). Transition of surface energy budget in the Gobi desert between spring and summer seasons. *Journal of Climate and Applied Meteorology*, **25**: 1725–1740.
- Smith, R.K. (1988). Travelling waves and bores in the lower atmosphere: the 'Morning Glory' and related phenomena. *Earth-Science Reviews*, **25**: 267–290.
- Smith, R.K., Reeder, M.J., Tapper, N.J. & Christie, D.R. (1995). Central Australian cold fronts. *Monthly Weather Review*, **123**: 16–38.
- Smith, R.K. & Ridley, R.N. (1990). Subtropical continental cold fronts. *Australian Meteorological Magazine*, **38**: 191–199.
- Sun, J., Howell, J.F. & Esbensen, S.K. (1996). Scale dependence of air-sea fluxes over the western equatorial Pacific. *Journal of Atmospheric Sciences*, **53**: 2997–3012.
- Tapper, N.J. (1991). Evidence for a mesoscale thermal circulation over dry salt lakes. *Paleogeography, Paleoclimatology, Paleocology*, **84**: 259–269.
- Tapper, N.J. & Barta, T. (1992). Surface energy balance studies at heathlands, northern Cape York Peninsula. *Cape York Peninsula Scientific Expedition*, pp. 9–16.
- Wang, J. & Mitsuta, Y. (1992). Evaporation from the desert: Some preliminary results of HEIFE. *Boundary-Layer Meteorology*, **59**: 413–418.